Attenuation of atomic displacement damage in the heavy reflector of the PERLE experiment and application to EPR

Shengli Chen, David Bernard

Version of Record: https://www.sciencedirect.com/science/article/pii/S0029549319302225
Manuscript_ec0dfb17f3c514a7ddb63a92c3f17e85

Attenuation of atomic displacement damage in the heavy reflector of the PERLE experiment and application to EPR

Shengli Chen[1,2,*], David Bernard[1]

[1] CEA, Cadarache, DEN/DER/SPRC/LEPh, 13108 Saint Paul Les Durance, France

[2] Université Grenoble Alpes, I-MEP2, 38402 Saint Martin d'Hères, France

[*] Corresponding author: shengli.chen@cea.fr

Abstract

The investigation of atomic displacement damage is important for studying the irradiated materials. The present work proposes two equations to describe the total neutron-induced and gamma-induced Displacement per Atom (DPA) rates versus the penetration in materials. The attenuation of DPA rate in materials is studied in the heavy reflector of the PERLE experiment. The proposed analytic formula for neutron-induced atomic displacement well describes the Monte Carlo simulated results with two fitting parameters, while the formula for gamma-induced DPA is in agreement with Monte Carlo simulations with potential 10% uncertainties. It is noticeable that the neutron flux above 0.5 MeV is more representative than that above 0.1 MeV or 1 MeV for the attenuation of DPA in the heavy reflector. Due to the representativity of the PERLE experiment for the heavy reflector of Evolutionary Pressurized Reactor (EPR), an analytic expression of displacement damage is obtained. The atomic displacement rate on the inner surface of EPR heavy reflector is 1.4 DPA/year (using the standard Norgett-Robinson-Torrens (NRT)-DPA metric). The DPA rate at the outer surface of the reflector is reduced by a factor of 9 (and 32) as the thickness of the steel increases from 2 cm to 20 cm (and 30 cm).

Graphical abstract

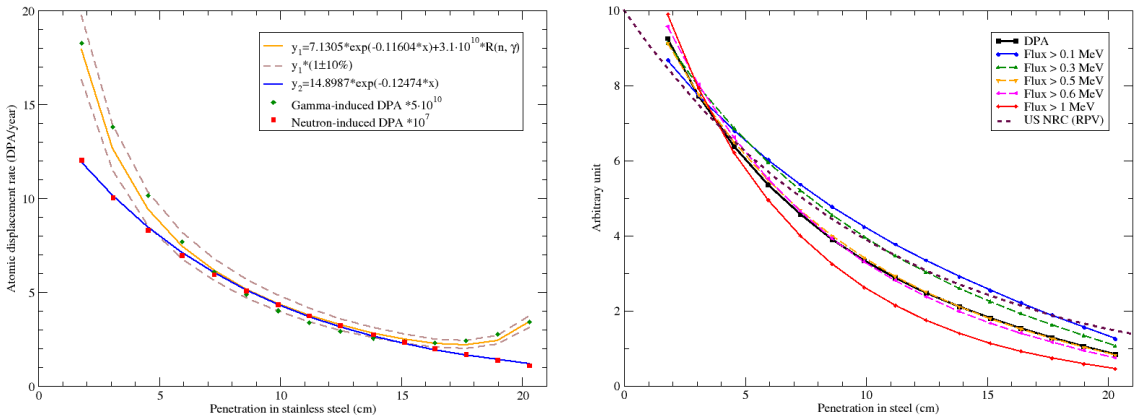

Keywords: PERLE, EPR, Displacement per Atom, Attenuation, Neutron flux, Gamma

1. Introduction

The studies on the irradiation-induced atomic displacement damage are of importance because it influences the features of materials under and after irradiation. The irradiation damage is estimated by the average number of Displacement per Atom (DPA). Neutron and photon flux are two important issues for producing the DPA in both the fuel cladding and the Reactor Pressure Vessel (RPV). The neutron-induced displacement damage cross sections can be processed by NJOY [1] with the corresponding Evaluated Nuclear Data File (ENDF). The reliability and potential improvements for the computation of DPA cross sections are shown in Refs. [2], [3].

In a reactor core, because neutrons are slowed down in the moderator, the relative importance of gamma-induced DPA increases with the distance from the core. For example, gamma-induced atomic displacement damage in the RPV of an Advanced Boiling Water Reactor (ABWR) is about 50% or even more of the neutron-induced DPA [4], [5]. Alexander [6] used the modified Kinchin-Pease (KP) DPA formula [7]. If the standard Norget-Robinson-Torrens (NRT) DPA metric [8] is applied, the gamma-induced DPA investigated in Refs. [4], [5] should be around 0.8 times (Robinson's partition function [9] is equal to 0.87 for 100 eV iron and 0.75 for 15 MeV electron or positron produced by gamma-ray) the computed results. Anyway, 40% of the neutron-induced DPA is still important for the irradiation damage.

In addition, the gamma-induced DPA can be more important than the neutron-induced DPA in Hight Flux Isotope Reactor (HFIR) surveillance [10] (although the former should be divided by a factor of about 1.5 to correct Baumann's gamma-induced KP-DPA cross sections [11] by the recent recommended photon-induced NRT-DPA cross sections [12]). It is shown that the gamma-induced damage provokes the accelerated embrittlement of the HFIR RPV [13].

DPA is a key parameter to measure the primary damage of materials under irradiation. However, due to the attenuation of the quantities of particles in materials, the DPA rate varies with the distance from the surface of fuel cladding, reflector, and RPV. The present work focuses on the investigation of attenuation of the DPA rate in stainless steel, which is the material used for the RPV, the fuel cladding in fast reactors, and potential fuel cladding of accident tolerant fuel in light water reactors [14], [15]. The studies are performed with the Programme d'Etude du Réflecteur Lourd dans Eole (PERLE) experiment [16], [17], of which the heavy reflector is used to study the attenuation of deposited gamma dose and the neutron flux. More details are presented in Section 2.1.

The main objective of the PERLE experiment is to study the heavy reflector in Evolutionary Pressurized Reactor (EPR). Because of the representativity of the PERLE reflector for the heavy of EPR, the results obtained in the PERLE experiment are used to determine the atomic displacement damage of the EPR heavy reflector. The methods are explained in Section 2.3 and the results are shown in Section 3.4.

2. Description of the models

2.1 Description and modeling of the PERLE experiment

2.1.1 Validation of calculations

The configuration of the PERLE experiment is shown in Figure 1. The core is fueled by standard 3.7% enrichment UO_2 fuel with Zircaloy-4 cladding. The moderator-to-fuel ratio is 1.7. Calculations and experiment are performed at room temperature, i.e. 294 K. Ref. [18] shows the limitation of gas model for describing the Doppler effect, whereas only the gas model is available in NJOY [1] processing code for the Doppler broadening. The effective fuel temperature by accounting for the crystal lattice vibration effect is given by [18]:

$$T_{eff} = T + 8.6 + 3100/T, \quad (1)$$

where T and T_{eff} are in Kelvin. Therefore, the effective fuel temperature used in the simulation of the PERLE core is 313 K.

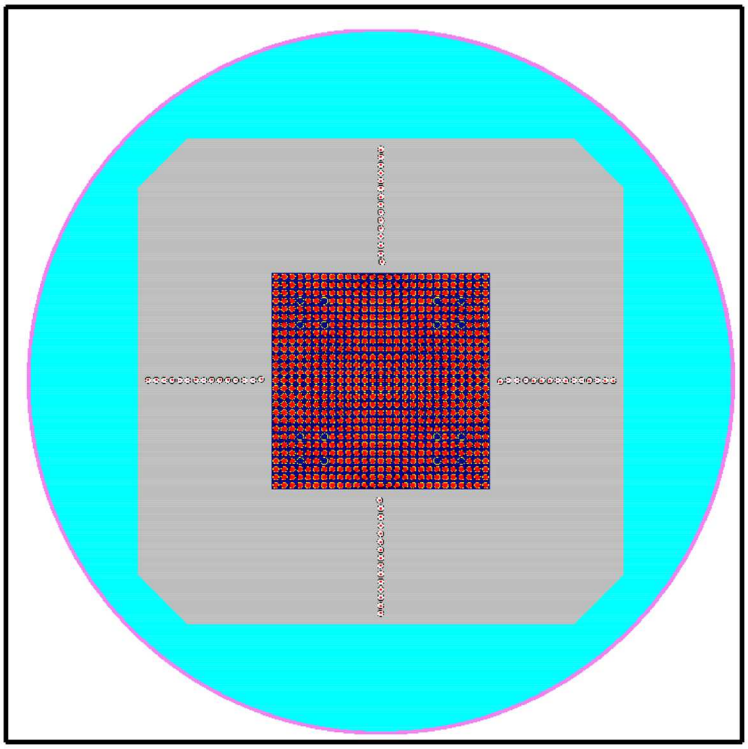

Figure 1. Configuration of the PERLE experiment with additional symmetric hollows

The calculations are performed with the Monte Carlo code Tripoli-4.10® [19] using JEFF-3.1.1 [20] nuclear data library. The simulations for $T_{eff} = 314$ K ($T = 294$ K resp.) give the reactivity and corresponding statistical uncertainty of 136 ± 4 pcm (205 ± 2 pcm resp.). Consequently, the Doppler coefficient of the PERLE core is -3.5 ± 0.3 pcm/K. The calculated reactivity for $T_{eff} = 313$ K based on Monte Carlo transport is 139 ± 4 pcm, which is in good agreement with experimental result 154 ± 22 pcm [17]. Both the analysis of reactivity performed in the present work and the results of pin-by-pin power distributions and detector responses studied in Ref.

[17] show the reliability of calculations performed with Tripoli-4.10® and JEFF-3.1.1. In addition, JEFF-3.1.1 based Tripoli-4 calculations of relative doses in the heavy reflector are in good agreement with the doses measured by Thermo-Luminescent Dosimeter (TLD) [21]. Therefore, the calculations performed with Tripoli-4 Monte Carlo simulations using JEFF-3.1.1 are validated against the experimental measurements.

2.1.2 Description and modeling of the heavy reflector

The PERLE experiment was performed in the CEA zero-power reactor EOLE. One of the main objectives of the PERLE experiment is providing representative experimental data for stainless steel reflector, which is used in Generation III reactors, such as Evolutionary Pressurized Reactor (EPR) [22] and Water Water Energy Reactor (VVER)-1000. The heavy reflector of the PERLE experiment has 22 cm thickness and about 5600 pcm reactivity worth.

As shown in Figure 1, there are 15 hollows at the center of each block of the heavy reflector. In fact, as shown in Figure 2(b) in Ref. [17], this kind of hollows are only in one block for measurements. Due to the symmetry of geometry, the present work adds these hollows in the other blocks so that the convergence of statistic score is accelerated. In addition, because the present work focuses on the attenuation of PDA rate in the reflector, the flux in each hollow above the uppermost dosimetry and below the lowermost dosimetry is also accounted for. The positions of hollows are referred to P1 to P15 from inside to outside hereinafter.

2.2 Attenuation of DPA

For convenience, the penetration in the material is denoted by x. As shown in Figure 2, following the path from the penetration x to $x+dx$, the concentration n obeys the law of conservation:

$$n(x+dx) = n(x) - n(x)\Sigma dx + S(x), \tag{2}$$

where Σ is the macroscopic reaction cross section and $S(x)$ is the source. The finite difference of concentration is $dn(x) = n(x+dx) - n(x)$. Accordingly,

$$n'(x) + n(x)\Sigma - S(x) = 0. \tag{3}$$

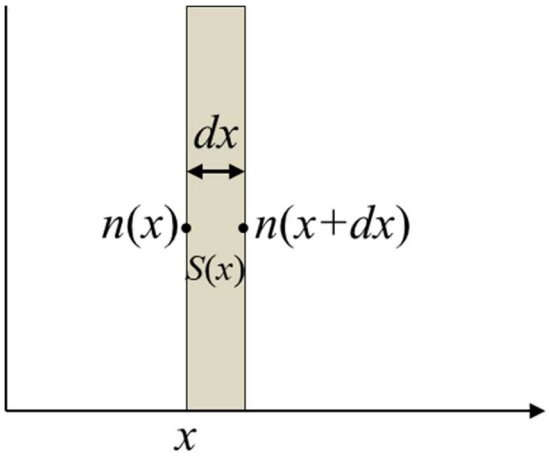

Figure 2. Scheme of particle density in material

Because there is no neutron source in the reflector (without considering the (γ, n) reaction), the neutron flux obtained by solving Eq. (3) is:

$$\phi_n(E, x) = \phi_{n0}(E) e^{-\Sigma_n(E)x}, \tag{4}$$

where $\phi_{n0}(E) \equiv \phi_n(E, 0)$ and the subscript *n* represents neutron. Because the DPA rate is integrated over the incident energy, the following investigations are based on 1-group energy structure. Defining the 1-group macroscopic cross section as Σ_n, the flux in the reflector becomes:

$$\phi_n(x) = \phi_{n0} e^{-\Sigma_n x}. \tag{5}$$

For a given spectrum, the atomic displacement is proportional to the number of incident particles. Consequently, the distribution of DPA rate versus the penetration has the following form:

$$DPA_n(x) = DPA_{n0} e^{-\Sigma_n^{DPA} x}. \tag{6}$$

Σ_n^{DPA} is not necessary equal to Σ_n because DPA depends on both the neutron quantities and neutron energy.

Due to the contribution of (n, γ) reaction, the source term $S(x)$ should be taken into account for the computation of gamma flux in the reflector. A particular solution of Eq. (3) is:

$$n_p(x) = \left[\int_0^x S(x') e^{\Sigma x'} dx' - C\right] e^{-\Sigma x}, \tag{7}$$

where *C* is arbitrary. To simplify the expression, one can choose the constant *C* that the constant term in the bracket is null.

If the (n, γ) reaction rate $R(n, \gamma)$ versus the penetration has an exponential form, a particular solution of Eq. (3) is proportional to the $R(n, \gamma)$. By Analogy to the neutron-induced DPA given in Eq. (6), the gamma-induced DPA rate is:

$$DPA_\gamma(x) = A e^{-\Sigma_\gamma^{DPA} x} + B R(n, \gamma)(x), \tag{8}$$

where *A* and *B* are constant, the subscript γ represents gamma. In fact, $R(n, \gamma)(x)$ is not an exponential function due to the increase of thermal neutrons shown in Figure 3 and Figure 4. However, in order to avoid introducing too many parameters to describe the gamma-induced DPA versus the penetration, Eq. (8) is applied with potential uncertainties. The accuracy of Eq. (8) for the gamma-induced DPA rates are described in Section 3.2.

One of the advantages of using Eqs. (6) and (8) are the simple form of atomic displacement versus the penetration. In addition, the explicit expression of DPA leads to the direct transformation between the position-dependent and volume-integrated displacement damage. Taking the neutron-induced DPA as an example, the volume-averaged displacement damage is equivalent to:

$$\overline{DPA_n} = \frac{DPA_{n0}}{\Sigma_n^{DPA}(x_2 - x_1)} \left(e^{-\Sigma_n^{DPA} x_1} - e^{-\Sigma_n^{DPA} x_2}\right), \tag{9}$$

where x_1 and x_2 are the penetration of two boundaries of the considered volume. According to Eq. (9), two volume-averaged DPA rate can be used to determine the neutron-induced DPA rate at any position using Eq. (6). If the inner surface of the

considered volume is the surface facing the core, i.e. $x_1 = 0$,

$$\overline{DPA_n} = \frac{DPA_{n0}}{\Sigma_n^{DPA} x_2}\left(1 - e^{-\Sigma_n^{DPA} x_2}\right). \quad (10)$$

Comparing with the position-dependent DPA rate at each position, the volume-averaged DPA rate has smaller uncertainties because of more available data. For instance, the statistical uncertainties are inversely proportional to the number of independent samples. In addition, due to the decrease of flux versus the penetration in the case of no source, the relative statistical uncertainties of atomic displacement increase with the penetration. In this case, the present work recommends using Eq. (10) so that the uncertainties of parameters in Eq. (6) can be largely decreased.

2.3 From PERLE to EPR

As shown in Figure 1, the PERLE experiment is fueled by 713 (27×27 lattice with 16 holes) fuel pins of which the active height is 80 cm. The stable thermal power during measurements is about 10 W. Both 3.6% enrichment UO_2 fuel and 1.7 moderator-to-fuel ratio of the PERLE experiment are representative of a typical Pressurized Water Reactor (PWR). The heavy reflector of the PERLE experiment encloses the core. This design is used to study the properties of the heavy reflector of EPRs.

The neutron flux in EPR is larger than that in the PERLE experiment by a factor of 9.60×10^5. Because of the representativity of the PERLE experiment for the heavy reflector of EPR, the results determined in the PERLE heavy reflector and the above two factors can give reasonable conclusions for the heavy reflector in EPRs.

3. Results and discussion

3.1 Attenuation of neutron flux and gamma flux

The neutron spectra at the penetration of 1.79 cm, 7.26 cm, 13.84 cm, and 20.28 cm (referred to P1, P5, P10, and P15, respectively) are shown in Figure 3. The dips of neutron spectra are due to the resonances of reaction cross sections, such as the large resonance of elastic scattering of ^{56}Fe at 29.7 keV. In general, the neutron flux decreases with the penetration in the reflector because of the reactions of neutrons with materials. It is noticeable that the thermal neutron flux increases with the penetration at depths greater than P10 (shown in Figure 4). This increase of thermal neutron is mainly due to the albedo from moderator surrounding the reflector. However, because the thermal neutrons cannot produce displacement damage through scattering reactions and the negligible contribution of neutron capture reaction-induced atomic displacement [23], the variations of thermal neutrons has limited influence on the DPA rate.

The photon spectra at the penetration of P1, P5, P10, and P15 are shown in Figure 5. From the surface facing the core to P10, the gamma flux decreases with the penetration in the reflector due to the predominant role of gamma-matter interactions. Nevertheless, the gamma flux is not a monotone function of the penetration from P10. The (n, γ) reaction in the reflector produces photons. Figure 4 plots both the neutron

spectra from P11 to P15 and the (n,γ) reaction cross section of ^{56}Fe. The (n,γ) reaction cross section is significant at the thermal region, in which the neutron flux increase with the penetration in the reflector. Therefore, the gamma production increases with the penetration in the reflector at depths greater than P10.

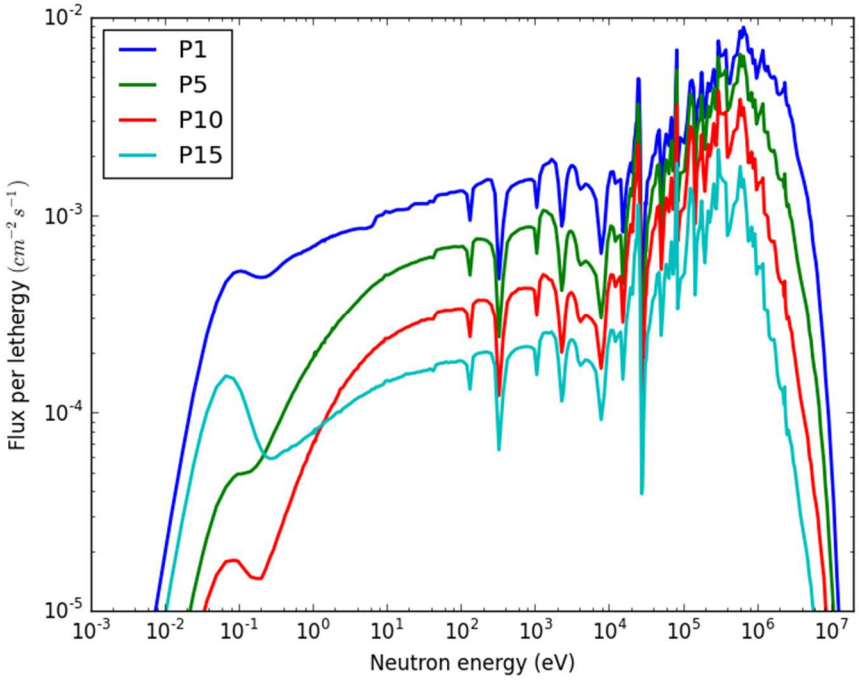

Figure 3. Neutron spectra in the reflector of PERLE

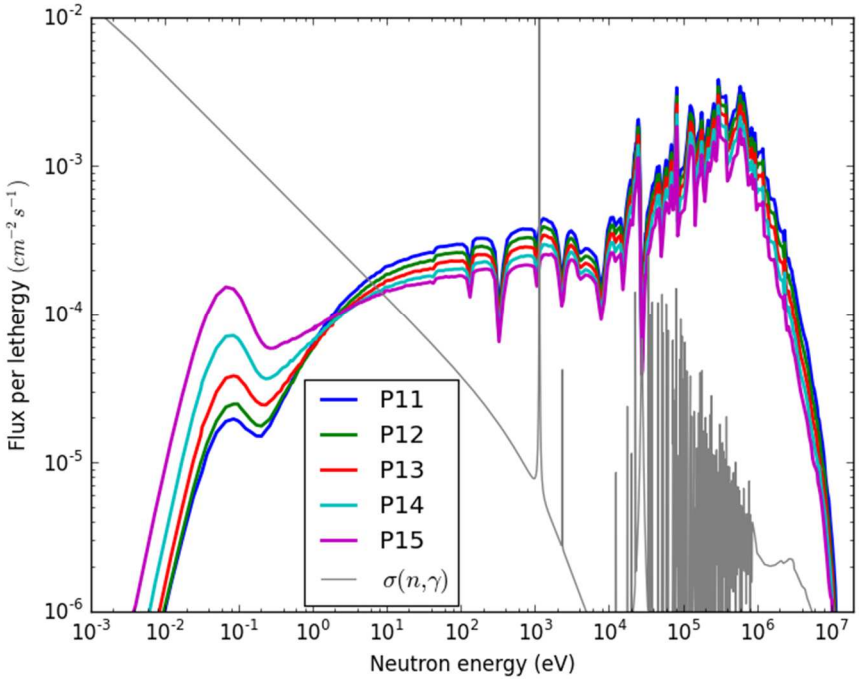

Figure 4. Neutron spectra in the reflector from P11 to P15. The grey curve represents the neutron radiative capture cross section of ^{56}Fe with arbitrary unit.

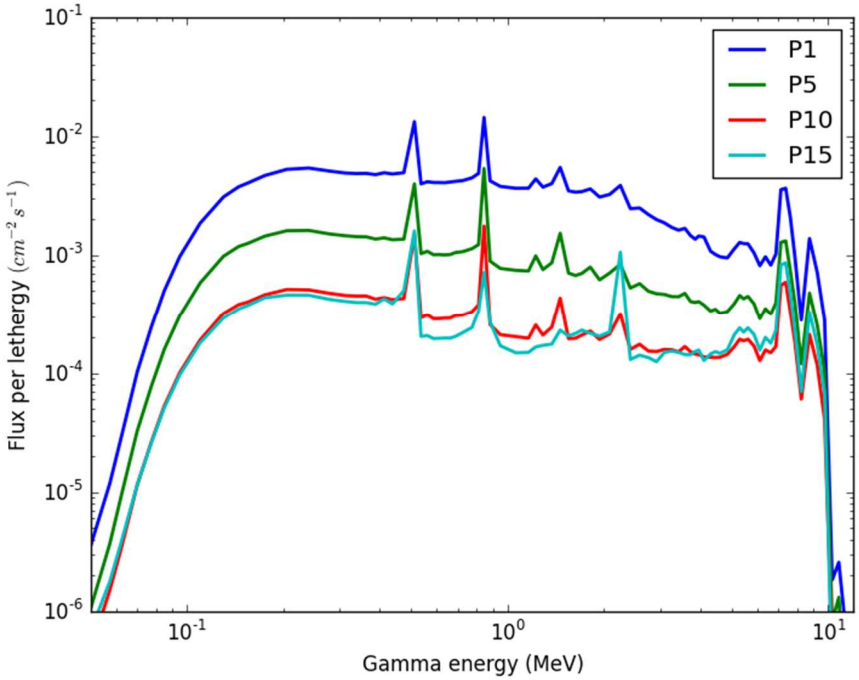

Figure 5. Photon spectra in the reflector of PERLE

3.2 Attenuation of DPA rate

With the neutron and photon spectra computed with Tripoli-4.10® Monte Carlo simulations, the total DPA rates in the reflector are calculated using the total neutron-induced DPA cross section processed by NJOY [1] and the total gamma-induced DPA cross section recommended in Ref. [12] and tabulated in Table I. The methods for DPA calculations with DPA cross sections and incident spectra are given in Ref. [23]. The total atomic displacement damage induced by neutrons and photons are plotted in Figure 6 with scattered points. The uncertainties from the statistical uncertainties are controlled by the simulated neutrons number and batches number. The uncertainties of neutron-induced (gamma-induced resp.) DPA due to the statistical uncertainties are within 0.5% (from 0.7% to 1.8% resp.).

Table I. Total gamma-induced DPA cross section of ^{56}Fe

E_γ(MeV)	σ_{DPA} (barn)	E_γ(MeV)	σ_{DPA} (barn)	E_γ(MeV)	σ_{DPA} (barn)	E_γ(MeV)	σ_{DPA} (barn)
0.63	0.00	5.50	1.488	10.50	4.655	15.50	8.784
1.00	0.0057	6.00	1.748	11.00	5.033	16.00	9.233
1.50	0.0464	6.50	2.022	11.50	5.419	16.50	9.687
2.00	0.1395	7.00	2.309	12.00	5.814	17.00	10.147
2.50	0.2699	7.50	2.609	12.50	6.217	17.50	10.612
3.00	0.4266	8.00	2.921	13.00	6.628	18.00	11.081
3.50	0.6045	8.50	3.247	13.50	7.046	18.50	11.554
4.00	0.8007	9.00	3.583	14.00	7.470	19.00	12.030
4.50	1.014	9.50	3.930	14.50	7.902	19.50	12.510
5.00	1.244	10.00	4.287	15.00	8.339	20.00	12.995

For neutron-induced DPA, the fitting of Monte Carlo simulated results using Eq. (6) are plotted in Figure 6 by the blue curve. The good agreement with Monte Carlo based calculations and the fitting curve shows the availability of Eq. (6) for describing the neutron-induced atomic displacement. In addition, the validation of Eq. (6) points out 1.5×10^{-6} DPA/year atomic displacement damage at the surface of the reflector facing the PERLE core. The equivalent macroscopic cross section for neutron-induced DPA is $\Sigma_n^{DPA} = 0.125\ \text{cm}^{-1}$.

As explained in Section 3.1, the increase of gamma-induced DPA in Figure 6 is due to the increase of thermal neutron-induced (n,γ) reaction of ^{56}Fe. Results in Figure 6 shows that Eq. (8) cannot describe the gamma-induced atomic displacement as well as Eq. (6) for neutron-induced DPA. The least squared fitted curve (orange curve in Figure 6) has discrepancies with the Monte Carlo based simulations. However, the discrepancies are within 10%, illustrated by the dashed brown curves in Figure 6. Therefore, the analytic expression

$$DPA_\gamma(x) = 1.426 \times 10^{-10} e^{-0.116x} + 0.62R(n,\gamma)(x). \qquad (11)$$

describes the gamma-induced DPA rate in the heavy reflector of the PERLE experiment with potential 10% uncertainties. In the heavy reflector, Figure 6 shows that the gamma-induced DPA rate is lower than that induced by neutron by a factor of about 5000. Nevertheless, it is noteworthy that the gamma-induced DPA is not negligible in BWR RPV [4], [5] and becomes more important than the neutron-induced DPA in HFIR surveillance [10].

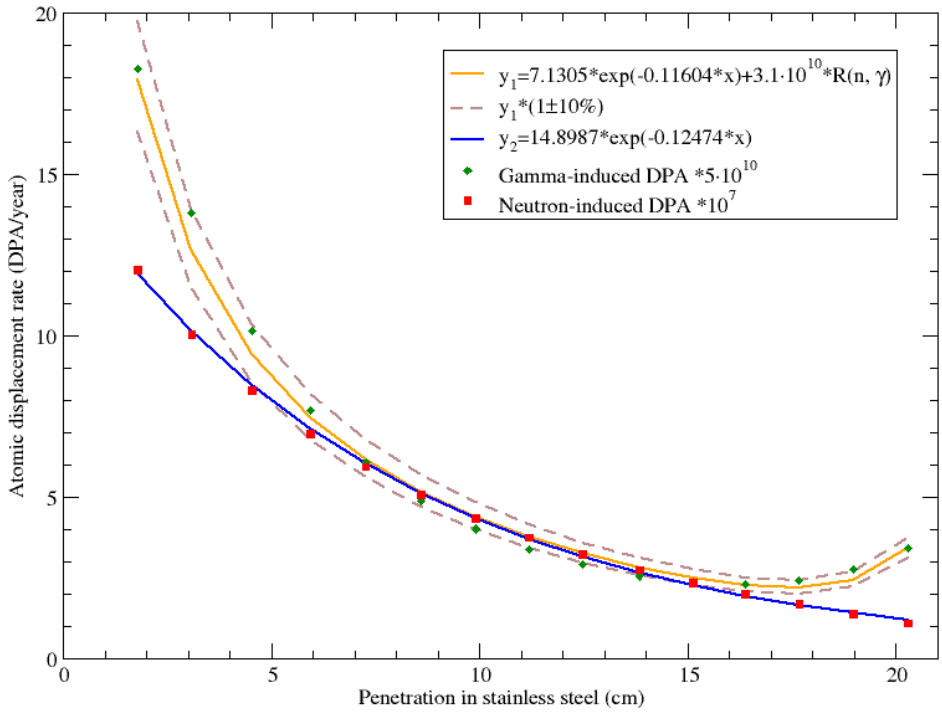

Figure 6. DPA rates in the heavy reflector of the PERLE experiment

3.3 Comparison of DPA with neutron flux

In applications, the DPA of materials is often deduced from the neutron fluence because the latter is much easier to measure. In order to examine the representativity of neutron fluence for DPA, the DPA rates and neutron flux in the heavy reflector are compared. Figure 7 shows the DPA rates and neutron flux in the heavy reflector. The quantities in Figure 7 are renormalized by different constants for visual comparisons. Even if the DPA rates are based on the NRT formula, the attenuation is similar to the molecular dynamics simulations [24]. From Figure 7, one can find that the sum of neutron flux above 1 MeV attenuates stronger than that of DPA rate, while the flux above 0.1 MeV has a slower attenuation than DPA rate. In the heavy reflector, the neutron flux above 0.5 MeV is shown representative of DPA rates, whereas the neutron fluence with energy higher than 1 MeV is the most common measure for mechanical property changes for metals and alloys [25]. Therefore, it is quite reasonable to use neutron fluence with energy higher than 0.5 MeV for studying the embrittlement of RPV materials [26]. In the heavy reflector, the relationship between DPA and neutron fluence above 0.5 MeV $\phi_{0.5}$ is:

$$\mathrm{DPA} = C\phi_{0.5}, \tag{12}$$

where the constant $C = 8.6 \times 10^{-22}$ $\mathrm{DPA}/(\mathrm{n} \cdot \mathrm{cm}^{-2})$.

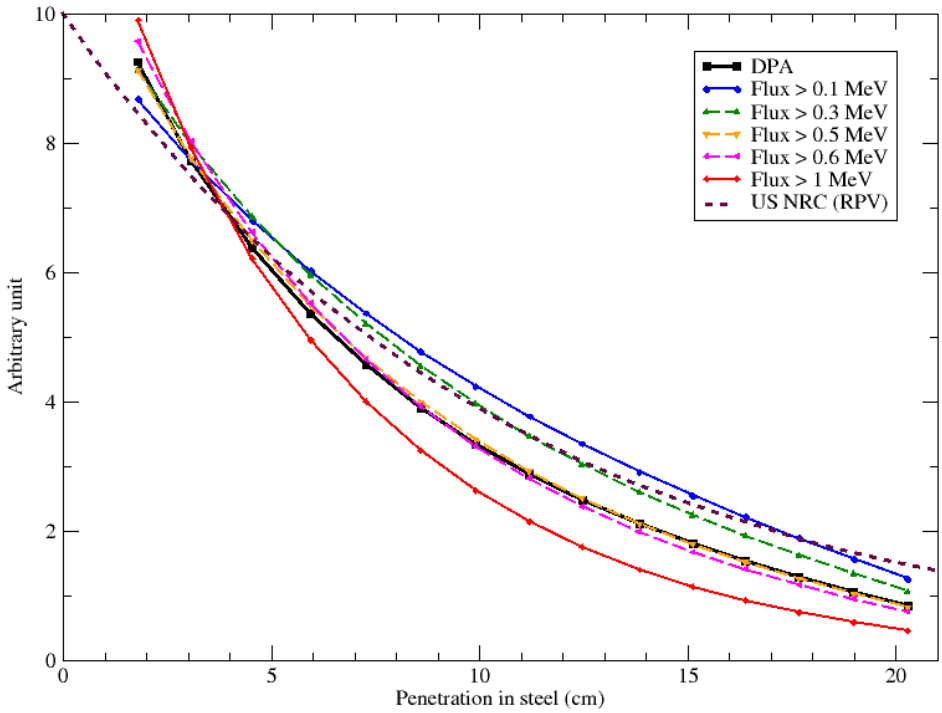

Figure 7. DPA rates and neutron flux in the heavy reflector with arbitrary renormalizations

For comparison, Figure 7 also shows the US Nuclear Regulatory Commission (NRC)'s formula for the attenuation of neutron flux above 1 MeV in the reactor vessel [27]. One can evidently observe that the DPA rate and the neutron flux above 1 MeV in the heavy reflector decrease much more quickly with the depth of penetration than

the US NRC's formula. It is noteworthy that Refs. [28], [29] also shows the neutron flux with energy above 1 MeV decrease more quickly than the DPA in PWR RPV than the formula proposed in the regulatory guide of NRC.

3.4 Atomic displacement in the EPR heavy reflector

According to the results in Section 3.2, the gamma-induced atomic displacement damage is negligible. The total atomic displacement is equivalent to the neutron-induced displacement damage:

$$D(x) = 1.42e^{-0.12426x} \text{ [DPA/year]}, \quad (13)$$

where x is in cm. The atomic displacement on the inner surface of the heavy reflector of EPR is 1.42 DPA/year. The values of $D(x)$ and the average atomic displacements from the inner surface to the penetration x in the reflector of EPR are given in Table II. If the attenuation of DPA rate in a 2 cm steel reflector or baffle, which is used in current French Gen II PWR, follows the same law as Eq. (13), the DPA rate at the outer surface of steel baffle can be reduced by a factor of 9.4 (32.4 resp.) when a 2 cm baffle is replaced by a 20 cm (30 cm resp.) heavy reflector in EPR. Therefore, the radiation damage in the RPV of EPR can be largely reduced due to the heavy reflector.

Table II. $D(x)$ and the average DPA rate in the heavy reflector of EPR from the inner surface to the penetration x

x (cm)	0.1	0.5	1	2	5	10	20	30
$D(x)$	1.40	1.34	1.25	1.11	0.763	0.410	0.118	0.034
Average	1.41	1.38	1.34	1.26	1.06	0.813	0.524	0.372

4. Conclusions

The interpretation of the PERLE experiment is validated against the experimental results of pin-by-pin power distributions [17], deposited gamma dose in the reflector [21], and the residual reactivity (Section 2.1.1 of the present work). Therefore, the heavy reflector of the PERLE experiment is used to study the attenuation of atomic displacement damage in materials using the Monte Carlo simulated results. By analogy of the attenuation of flux in materials, the present work proposes two simple equations for describing the total neutron-induced and gamma-induced DPA rates versus the penetration in materials.

Due to the lack of neutron source in the reflector, the neutron flux decreases with the penetration in stainless steel. A noticeable effect is the increase of thermal neutrons from the penetration position of 14 cm. Because the contribution of thermal neutrons on neutron-induced DPA is negligible, the neutron-induced atomic displacement in the heavy reflector of the PERLE experiment can be well described by the exponential law proposed in the present work. However, because the thermal neutrons are important for producing photons through the (n,γ) reaction, the gamma-induced DPA rate increases with the penetration in stainless steel from 15 cm.

The proposed formula for gamma-induced atomic displacement is validated against the Monte Carlo simulations within 10% uncertainties. It is also found that the neutron flux above 0.5 MeV is more representative than that above 0.1 MeV or 1 MeV for the attenuation of DPA in heavy reflector.

According to the validated analytic approach of atomic displacement of the PERLE experiment, an explicit formula of displacement damage of the heavy reflector of EPR is obtained as a function of the penetration. 1.4 DPA/year irradiated displacement damage rate is determined in the inner surface of EPR heavy reflector. Comparing with 2 cm thick steel baffle, the 20 cm (30 cm resp.) thick heavy reflector can reduce DPA rate at the outer surface of reflector by a factor of about 9 (32 resp.).

Acknowledgments

The authors acknowledge Dr. Claire Vaglio-Gaudard and Dr. Simon Ravaux for their works on the interpretation of the PERLE experiment.

References

[1] R. E. MacFarlane and A. C. Kahler, "Methods for Processing ENDF/B-VII with NJOY," *Nucl. Data Sheets*, vol. 111, no. 12, pp. 2739–2890, Dec. 2010.

[2] S. Chen, D. Bernard, P. Tamagno, J. Tommasi, S. Bourganel, and G. Noguere, "Irradiation Damage Calculation with Angular Distribution," *arXiv*, no. 1902.05620, 2019.

[3] S. Chen and D. Bernard, "Relativistic effect on two-body reaction inducing atomic displacement," *J. Nucl. Mater.*, vol. 522, pp. 236–245, Aug. 2019.

[4] D. E. Alexander and L. E. Rehn, "The contribution of high energy gamma rays to displacement damage in LWR pressure vessels," *J. Nucl. Mater.*, vol. 209, no. 2, pp. 212–214, Apr. 1994.

[5] D. E. Alexander and L. E. Rehn, "Gamma-ray displacement damage in the pressure vessel of the advanced boiling water reactor," *J. Nucl. Mater.*, vol. 217, no. 1, pp. 213–216, Nov. 1994.

[6] D. E. Alexander, "Defect production considerations for gamma ray irradiation of reactor pressure vessel steels," *J. Nucl. Mater.*, vol. 240, no. 3, pp. 196–204, Feb. 1997.

[7] G. H. Kinchin and R. S. Pease, "The Displacement of Atoms in Solids by Radiation," *Rep Prog Phys*, vol. 18, no. 1, pp. 1–51, 1955.

[8] M. J. Norgett, M. T. Robinson, and I. M. Torrens, "A proposed method of calculating displacement dose rates," *Nucl. Eng. Des.*, vol. 33, no. 1, pp. 50–54, 1975.

[9] M. T. Robinson, "Energy Dependence of Neutron Radiation Damage in Solids," *Nucl. Fusion React.*, pp. 364–378, 1970.

[10] I. Remec, J. A. Wang, F. B. K. Kam, and K. Farrell, "Effects of gamma-induced displacements on HFIR pressure vessel materials," *J. Nucl. Mater.*, vol. 217, no. 3, pp. 258–268, Dec. 1994.

[11] N. P. Baumann, "Gamma-ray Induced Displacements in D2O Reactors," in

Proceedings of the Seventh ASTM-EURATOM Symposium on Reactor Dosimetry, Strasbourg, France, 1990, pp. 689–697.

[12] S. Chen, D. Bernard, and C. De Saint Jean, "Calculation and analysis of gamma-induced irradiation damage cross section," *Nucl. Instrum. Methods Phys. Res. Sect. B Beam Interact. Mater. At.*, vol. 447, pp. 8–21, May 2019.

[13] K. Farrell, S. T. Mahmood, R. E. Stoller, and L. K. Mansur, "An evaluation of low temperature radiation embrittlement mechanisms in ferritic alloys," *J. Nucl. Mater.*, vol. 210, no. 3, pp. 268–281, Jun. 1994.

[14] S. Chen and C. Yuan, "Neutronic Analysis on Potential Accident Tolerant Fuel-Cladding Combination U_3Si_2-FeCrAl," *Sci. Technol. Nucl. Install.*, vol. 2017, no. 3146985, 2017.

[15] S. Chen, C. Yuan, and D. Guo, "Radial distributions of power and isotopic concentrations in candidate accident tolerant fuel U_3Si_2 and UO_2/U_3Si_2 fuel pins with FeCrAl cladding," *Ann. Nucl. Energy*, vol. 124, pp. 460–471, Feb. 2019.

[16] A. Santamarina *et al.*, "The PERLE experiment for the qualification of PWR heavy reflectors," in *Proc. of Int. Conf. on the Physics of Reactors: Nuclear Power: A Sustainable Resource (PHYSOR2008)*, Interlaken, Switzerland, 2008.

[17] C. Vaglio-Gaudard *et al.*, "Interpretation of PERLE Experiment for the Validation of Iron Nuclear Data Using Monte Carlo Calculations," *Nucl. Sci. Eng.*, vol. 166, no. 2, pp. 89–106, Oct. 2010.

[18] A. Meister and A. Santamarina, "The Effective Temperature for Doppler Broadening of Neutron Resonances in UO_2," presented at the International Conférence on the physics of nuclear science and technology, New York, 1988, vol. 1.

[19] E. Brun *et al.*, "TRIPOLI-4®, CEA, EDF and AREVA reference Monte Carlo code," *Ann. Nucl. Energy*, vol. 82, pp. 151–160, Aug. 2015.

[20] A. Santamarina *et al.*, "The JEFF-3.1.1 Nuclear Data Library," OECD/NEA, JEFF Report 22, NEA No. 6807, 2009.

[21] S. Ravaux, "Qualification du Calcul de l'Échauffement Photonique dans les Réacteurs Nucléaires," Université de Grenoble, 2013.

[22] G. Sengler, F. Forêt, G. Schlosser, R. Lisdat, and S. Stelletta, "EPR core design," *Nucl. Eng. Des.*, vol. 187, no. 1, pp. 79–119, Jan. 1999.

[23] S. Chen, D. Bernard, and L. Buiron, "Study on the self-shielding and temperature influences on the neutron irradiation damage calculations in reactors," *Nucl. Eng. Des.*, vol. 346, pp. 85–96, May 2019.

[24] R. E. Stoller, "Evaluation of neutron energy spectrum effects and RPV thru-wall attenuation based on molecular dynamics cascade simulations," *Nucl. Eng. Des.*, vol. 195, no. 2, pp. 129–136, Feb. 2000.

[25] R. E. Stoller and G. R. Odette, "Recommendations on damage exposure units for ferritic steel embrittlement correlations," *J. Nucl. Mater.*, vol. 186, no. 2, pp. 203–205, Jan. 1992.

[26] B. Z. Margolin, E. V. Yurchenko, A. M. Morozov, N. E. Pirogova, and M. Brumovsky, "Analysis of a link of embrittlement mechanisms and neutron flux effect as applied to reactor pressure vessel materials of WWER," *J. Nucl. Mater.*,

vol. 434, no. 1, pp. 347–356, Mar. 2013.

[27] Office of Nuclear Regulatory Research, "Radiation Embrittlement of Reactor Vessel Materials," U.S. Nuclear Regulatory Commission, Regulatory Guide 1.99, Rev. 2, May 1988.

[28] R. Stoller and L. Greenwood, "An Evaluation of Through-Thickness Changes in Primary Damage Production in Commercial Reactor Pressure Vessels," in *Effects of Radiation on Materials: 20th International Symposium, ASTM STP 1405*, S. Rosinski, M. Grossbeck, T. Allen, and A. Kumar, Eds. American Society for Testing and Materials, West Conshohocken, PA, 2002.

[29] J. F. Carew and K. Hu, "Effect of Transverse Neutron Leakage on the Attenuation of the Displacements per Atom in the Reactor Pressure Vessel," *Nucl. Sci. Eng.*, vol. 152, no. 3, pp. 256–273, Mar. 2006.